Structural Monitoring and Maintenance, *Vol. 10, No. 2 (2023) 133-154*
https://doi.org/10.12989/smm.2023.10.2.133

A practical modification to coaxial cables as damage sensor with TDR in obscured structural members and RC piles

Mehmet Ozgur*[1] and Sami Arsoy[2a]

[1]*Deparment of Civil Engineering, Canakkale Onsekiz Mart University, Terzioglu Campus, Canakkale, Türkiye*
[2]*Department of Civil Engineering, Kocaeli University, Umuttepe Campus, Kocaeli, Türkiye*

(*Received April 28, 2023, Revised May 27, 2023, Accepted June 2, 2023*)

Abstract. Obscured structural members are mostly under-evaluated during condition assessment due to lack of visual inspection capability. Insufficient information about the integrity of these structural members poses a significant risk for public safety. Time domain reflectometry (TDR) is a novel approach in structural health monitoring (SHM). Ordinary coaxial cables "as is" without a major modification are not suitable for SHM with TDR. The objective of this study is to propose a practical and cost-effective modification approach to commercially available coaxial cables in order to use them as a "cable sensor" for damage detection with the TDR equipment for obscured structural members. The experimental validation and assessment of the proposed modification approach was achieved by conducting 3-point bending tests of the model piles as a representative obscured structural member. It can be noted that the RG59/U-6 and RG6/U-4 cable sensors expose higher strain sensitivity in comparison with non-modified "as is" versions of the cables used. As a result, the cable sensors have the capability of sensing both the presence and the location of a structural damage with a maximum aberration of 3 cm. Furthermore, the crack development can be monitored by the RG59/U-6 cable sensor with a simple calibration.

Keywords: cable sensor; coaxial cable; obscured structural members; RC pile; TDR

1. Introduction

Civil structures and infrastructures play a key role for the sustainable development of a country. As they age, knowledge of the actual response of these structures becomes more crucial for proactive maintenance and management processes, aiming to prolong the service life. The actual response of these structures may not be in accordance with the computed responses at the design stages due to various reasons such as idealization assumptions and unpredictable and changing nature of service loads (Park *et al*. 2007). Besides, some infrastructures may incorporate novel materials whose degradation processes are not well known and failures may occur even shortly after inaugurations (Rizzo and Enshaeian 2021). It is also well known that material degradation and structural damages can influence the structural response by means of stress, strain and deflection.

Human oriented visual inspection as a non-destructive evaluation (NDE) method can help to detect structural damages before they become critical to the overall stability of the structure

*Corresponding author, Ph.D., E-mail: mehmetozgur@comu.edu.tr
[a]Professor, E-mail: sarsoy@kocaeli.edu.tr

http://www.techno-press.org/?journal=smm&subpage=7 ISSN: 2288-6605 (Print), 2288-6613 (Online)

(Ellsworth and Ginnado 1991). However, the method has several shortcomings. It is time consuming, expensive and relies on an engineer's subjective, qualitative, or empirical knowledge (Yeum *et al*. 2018, Fils *et al*. 2021). Additionally, the method cannot be used for buried structures (i.e. culverts and buried pipes/pipelines) and obscured structural members (i.e., pile foundations) due to the lack of visual access. Thus, in most cases the obscured structural members such as foundations are under-evaluated during condition and risk assessment for maintenance and management purposes. However, there are strong evidences that foundations play essential role in the load carrying capacity, dynamic performance, and serviceability of bridges and in various other structures (Mao *et al*. 2019). For instance, NDE methods for the integrity assessment of the deep foundations (i.e., reinforced concrete (RC) piles) attracted significant interest and research effort in the last several decades with the enhancements in the modern technology. The NDE methods used for integrity assessment of RC piles can be classified mainly into three categories: (i) stress wave methods (sonic echo, impulse response, impedance logging, cross-hole sonic logging and parallel seismic test), (ii) nuclear method (gamma-gamma logging), and (iii) radar method (cross-hole ground penetrating radar).

Sonic echo method is based on tracking the transient stress wave introduced into the pile by striking the top of the shaft with an impulse hammer. The stress waves are reflected because of the impedance change, which may be caused by internal cracks. The capability of the method depends on the crack depth to the pile diameter ratio and the relative stiffness ratio between the pile and the soil (Huang *et al*. 2010). Gamma-gamma logging method includes a radioactive source and a counter which may be either in separate probes or housed in the same probe. The source is lowered down into a preplaced access tube or core-hole and raised slowly toward the surface. The radiation count increases with soil inclusion which is a sign of a crack on the pile (Baker *et al*. 1991). Possible health hazards and the requirement of an access tube or core-hole are the main drawbacks of this method. Cross-hole ground penetrating radar (GPR) uses a transmitting and receiving antenna which are placed in adjacent boreholes located at the two sides of the obscured structural member. The signal arrived at the receiving antenna stores important information about the structural member under investigation. The resulting waveform and the travel-time data of the cross-hole GPR can be difficult, complex and challenging to interpret (Qin *et al*. 2016). The advantages and disadvantages of the existing NDE methods for the integrity assessment of the deep foundations are summarized in Table 1.

NDE methods mentioned above used for obscured structural members require site/material specific calibrations and intensive computational effort, needing some time. Additionally, measured parameters can be subject to external influence from other parameters that may be known or unknown (Chen *et al*. 2022). However, in the case of an earthquake it is very important to detect and locate damages on the obscured structural members with adequate resolution in a reasonable time for public safety. Therefore, there is a need for an alternative NDE method with continuous monitoring capability, which can be integrated to a structural health monitoring (SHM) system. SHM provides useful information for determining the actual responses of structures or structural members by continuous measurement of a structure's operating and loading environment using spacial and temporal data, as well as critical responses to track and evaluate any symptoms of operational incidents, anomalies and deteriorations/damages, which might affect its actual response (Aktan *et al*. 2000, Brownjohn *et al*. 2011). Therefore, many infrastructure buildings and bridges have instrumented for SHM since the 1960s (Wang *et al*. 2020).

Time domain reflectometry (TDR) can be a promising alternative NDE method with its remote, real time and continuous monitoring capability. TDR is essentially a guided radar technology that has been widely used in electrical engineering since the 1930s for detection of breakages on the

Table 1 Advantages and disadvantages of the existing NDE methods

Method	Advantages	Disadvantages
Sonic echo	No requirement for pre-placed tubes Rapid measurement Relatively easy to interpret the data Portable equipment	Not usable for inaccessible pile head conditions Length (L) / Diameter (D) limitation: 50/1 for soft soils (Davis and Robertson 1976) and 30/1 for stiff clays (Hearne *et al*. 1981)
Impulse response	No requirement for pre-placed tubes Rapid measurement Moderate effort for data interpretation Portable and moderately complex equipment	Not usable for inaccessible pile head conditions L/D limitation Accuracy of damage depth is affected by the relative angle between the impact and defect (Ni and Huang 2013) Pile below severe cracks cannot be evaluated (Rausche *et al*. 1991)
Impedance logging	No requirement for pre-placed tubes Rapid measurement Portable and moderately complex equipment Pile shape can be determined	Not usable for inaccessible pile head conditions Substantial data analysis is required
Cross-hole sonic logging	Rapid measurement Accuracy of damage detection is higher than that of surficial stress wave methods No limitation for L/D	Surficial cracks cannot be detected Pre-placed or drilled tubes are required The success of the method depends upon the pile diameter, damage size and number of access tubes (Li *et al*. 2005)
Parallel seismic test	Usable for inaccessible pile head conditions No limitation for L/D	Requires a borehole close to the pile Accuracy of the method depends upon the pile length to borehole distance ratio and P wave velocity of the soil (Ni *et al*. 2011)
Gamma-gamma logging	Rapid measurement No limitation for L/D Accuracy of damage detection is higher than that of surficial stress wave methods	Pre-placed or drilled tubes are required Surficial cracks cannot be detected Possible health hazards due to nuclear radiation
Cross-hole ground penetrating radar	Usable for inaccessible pile head conditions No limitation for L/D	Requires a borehole close to the pile Substantial data analysis is required Accuracy of the method depends upon the soil water content, conductive properties of soil and the distance between borehole and pile (Chakraborty and Brown 1997)

cables (Cerny 2009) and their locations by sending and subsequently analyzing a pulsed electromagnetic (EM) signal into the conductors of the cable. TDR has been applied to a wide range of monitoring issues in civil engineering since the early 1980s, such as volumetric soil water content measurement (Topp *et al*. 1980, Ledieu *et al*. 1986, Malicki *et al*. 1996, Stangl *et al*. 2009, Arsoy *et al*. 2013), landslide monitoring (Lin *et al*. 2009), bridge scour monitoring (Yu and Yu 2011) and detection of corrosion of steel cables and reinforcing steel in concrete structures (Liu *et al*. 2002). Using TDR for structural damage detection has a shorter history with a limited literature.

In a pioneering study, Lin *et al*. (1999) used commercial coaxial cables as cable sensors with TDR for strain and crack sensing on structural members. The results of the bending tests that were

performed on small-scale concrete specimens with embedded coaxial cables demonstrated the great potential of the TDR for SHM applications. Although the cable sensor was able to capture the specimen deformation pattern and locate the cracks, they concluded that the inadequate signal-to-noise ratio (SNR) impaired the sensing capability of the method. Afterward, they replaced the tubular (teflon or polyethylene) insulating layer of the commercial coaxial cable with rubber to improve the sensitivity by facilitating the geometric change of the sensor cable. It was shown that the cable sensor with rubber insulating layer exposed 10 times higher strain sensitivity in comparison with a RG-174 commercial coaxial cable (Lin *et al*. 2000). Chen *et al*. (2004) designed a novel cable sensor with spiral shaped outer conductor. By this way, the sensing mechanism was based on the change in topology of the outer conductor instead of the change in geometry of the cable sensor. The bending test results of RC beams of 0.91 m long indicated that the topology-based cable sensors were 15–80 times more sensitive than sensors based on commercial coaxial cables. Chen *et al*. (2005) constructed a cable sensor with a new fabrication process to improve its performance consistency. The outer conductor of the new cable sensor was tin-plated, stainless steel commercial spirals and a solder cover. The cable sensor was implemented in a full-scale RC beam of approximately 15 m long for crack detection under a progressively increasing and cyclic torsional load. It was shown that the cable sensor was able to capture the most of the load induced cracks on the girder. Zhou *et al*. (2016) pointed that the spirally wrapped outer conductor of the cable sensors leads signal attenuation and limits the monitoring distance. They proposed a new topology-based cable sensor with a shallow helical groove on its external surface of the outer conductor. A computer numerical controlled milling machined was used to form the grooves where the key factor in the fabrication was to ensure that the grooves cannot cut through the outer conductor, but could be separated easily under loading. Experimental validation was performed on RC beams of 0.5 m long. The test results verified that the proposed sensor was able to locate the crack and detect the relative magnitude of the crack damage after a linear calibration.

In brief, the existing literature points out that the commercial coaxial cables cannot be used for damage detection of RC structural members with adequate resolution for SHM purposes without a major modification. The recent modifications require special cable sensor design and fabrication processes based on change in either geometry or topology. When the required monitoring length for obscured structural members is considered the existing modification alternatives cannot be referred as cost-effective.

The objective of this study is to propose a practical but a novel and economical modification approach to commercial coaxial cables in order to use them as a “cable sensor” for detecting damages on obscured structural members. The modification proposed consists of creating a series of circular notches on the protective jacket of the coaxial cables, and thereby allowing the longitudinal strain at the coaxial cable-concrete interface to be transferred directly on the outer conductor of the coaxial cable as a result of the discontinuity created by the circular notches. In other words, it is expected that increasing stresses in the concrete due to external loading may create varying sizes of cracks, which in turn induces longitudinal strains along the outer conductor that induces a reduction in the shielding capacity of the braided outer conductor. Because the interaction between the concrete and the outer conductor is proportional to one another, it will then become possible to assess the integrity of the concrete by monitoring the induced damage on the outer conductor of the coaxial cable via TDR device. In order to test the validity of the proposed approach, 3-point bending tests were conducted on the small-scale prismatic RC model piles representing an obscured structural member with 2 commonly available coaxial cables, RG59/U-6 and RG6/U-4 as cable sensors.

2. Background of TDR

TDR is a remote sensing method analogous to a closed circuit radar for detecting and locating impedance discontinuities in electronic systems, i.e. transmission lines (TLs). A typical TDR device basically consists of a high frequency step generator, a digitizing oscilloscope for signal sampling and display, and a signal TL (Lin and Thaduri 2006). There are some additional components which enables wireless communication, multiplexing and data storage in particular commercial models.

The TDR device generates a signal (hereafter called incident test wave), usually a step voltage with an ultra-short rise time and transmits it to the TL. While the pulse travels toward the TL, the magnitude of the reflected waves returning from the TL and their travel time are recorded. If there is no impedance discontinuity along the TL, the incident test wave should reflect back from the end of the TL without any loss. Otherwise, the reflected waves from the interface of the impedance discontinuity combines with the incident test wave and displayed by the TDR device. The TL used in this study is a coaxial cable.

Coaxial cable is a two conductor TL which consist of an inner and outer conductor separated by a tubular insulating layer with a high dielectric constant (Lin *et al*. 2009) and all of these components are encased by a protective jacket usually made out of polyvinyl chloride (PVC). An optional screen layer can also be under the outer conductor for extra protection. The characteristic impedance (Z_0) of the coaxial cable depends upon the permittivity (ε) and permeability (μ) of the insulating material and the geometrical configuration of the inner and outer conductors (Pozar 2012)

$$Z_0 = \sqrt{\frac{\mu}{\varepsilon}} \ \frac{\ln(b/a)}{2\pi} \tag{1}$$

where a and b are the diameters of the inner and outer conductors, respectively. When a local damage occurs on a coaxial cable which causes a change in its geometrical configuration, there will be a mismatch between the characteristic impedance and the impedance of the damaged point (fault) (Z_L). In such a case, some portion of the incident test wave reflects from the fault location. Then, the reflection coefficient (ρ) can be calculated as follows (Pozar 2012)

$$\rho = \frac{Z_L - Z_0}{Z_L + Z_0} \tag{2}$$

Signal losses must be considered for long TLs. Attenuation of the signal differs with the characteristics of the TL and the ρ must be recalculated with attenuation constant (A) according to (Castiglione and Shouse 2003)

$$\bar{\rho} = \frac{1}{A} \ \frac{Z_L - Z_0}{Z_L + Z_0} \tag{3}$$

where A relies on the length of the TL (l) and the attenuation coefficient (α) which is representing the residual cable loss due to the imperfect shielding, resistive conductors, signal absorption in the dielectric of the cable and non-uniform impedance profile of the cable (Large and Farmer 2009)

$$A = \exp(2\alpha l) \tag{4}$$

It is clear that the reflection coefficient is directly related with the level of the damage at the fault when the Eqs. (1) and (2) considered together. Inherently, the reflection coefficient is also a sign of the damage type. The ratio of b/a decreases when the coaxial cable is under tension forces, and the impedance at the fault becomes smaller than the characteristic impedance. Therefore, the reflection

coefficient has a negative value along the tensioned zone, which is called capacitive distortion (and vice versa for compression forces where inductive distortion occurs) (Lin *et al*. 2005). An inductive distortion also occurs in the presence of a discontinuity on the outer conductor, which introduces an additional inductance that leads to an increase in impedance. Location of the fault can be acquired by a travel time analysis by means of the distance between the TDR device and the fault (d)

$$d = \frac{1}{2} V_p t \tag{5}$$

where t is the travel time of the incident test wave forth and back from the TDR device to the fault location and (V_p) is the velocity of propagation of the incident test wave in the insulating layer along the cable which can be calculated by (Tektronix 2008)

$$V_p = \frac{c}{\sqrt{\varepsilon_r}} \tag{6}$$

where c is the speed of light in vacuum (2.998 x 10^8 ms^{-1}) and ε_r is the relative permittivity of the insulating material. Two neighboring discontinuities may only be distinguishable by a TDR device if there is a minimum spacing between them. This is called the spatial resolution (R) of the TDR device, and depends on the V_p and the rise time (t_r) of the incident test wave as follows (Tektronix 2008)

$$R = \frac{V_p t_r}{2} \tag{7}$$

3. Experimental method

3.1 Description of the TDR device

TDR measurements in this study were carried out by using TDR100 manufactured by Campbell Scientific, Inc. Amplitude and pulse length of the incident test wave were 0.25 volt into 50 ohms and 14 microseconds, respectively, while t_r was 300 picoseconds. The aberrations of undershooting and overshooting do not exceed $\pm$ 5.0% within the first 10 nanoseconds and $\pm$ 0.5% thereafter. The measurement range of the TDR100 is 2100 meters. In this study, waveform averaging was accomplished by collecting 30 values at a given distance before collecting values at the next distance increment in order to reduce noise level and obtain adequate SNR. Signal averaging with 30 repetitions improved the SNR by a factor of $\sqrt{30}$ (Hassan and Anwar 2010).

3.2 Description of the proposed cable sensor

Two types of commercial coaxial cables, RG59/U-6 and RG6/U-4, were used as the damage detection cable sensors in this study. Structural and electrical characteristics of the coaxial cables are summarized in Table 2.

In case of an embedded cable sensor, the ability of sensing depends on the level of strain transfer between the surrounding matrix, i.e., concrete and the sensor. Protective jacket significantly restrains the strain transfer between the concrete and the outer conductor of the cable due to its negligible friction with the outer conductor. In order to enhance the sensing capability, the coaxial cables were installed with a practical and simple modification as forming a series of circular notches on the

Table 2 Structural and electrical properties of the coaxial cables (Recber 2023)

Coaxial cable		RG59/U-6	RG6/U-4
Structure	Inner conductor	Copper	Copper
	Diameter of inner conductor (a)	0.8 mm	1.0 mm
	Insulating material	Foam polyethylene	Foam polyethylene
	Diameter of insulating layer	3.7 mm	4.6 mm
	Screen	Copper tape	Aluminum tape
	Outer conductor	Copper braid	Aluminum braid
	Sheath (protective jacket)	PVC	HFFR
	Total outer diameter	5.8 mm	6.8 mm
Electrical characteristics	Impedance (Z_0)	75 ± 3 ohm	75 ± 3 ohm
	Velocity of propagation (V_p)	0.82 ± 2% c	0.84 ± 2% c
	Attenuation coefficient (α) at 200 MHz	0.01Neper	0.01Neper

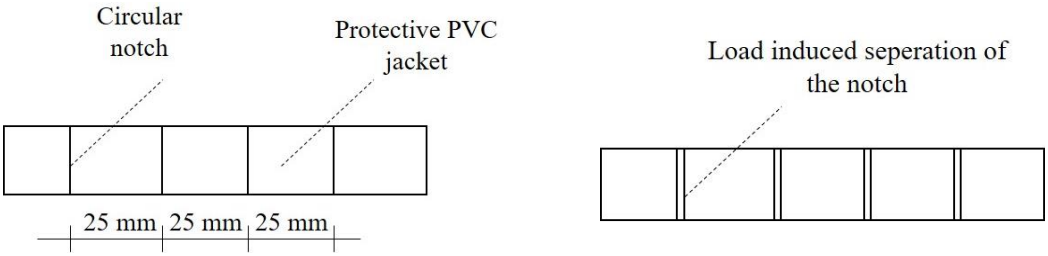

(a) Modification of the coaxial cable (b) Separation of the notch

Fig. 1 Schematic illustration of the cable sensor

protective jacket. Circular notches were formed by cutting the protective jacket with a special tool (Zupper TC-100). Load induced separation of the notches allows a direct strain transfer between the concrete and the outer conductor. Subsequently, the shielding effect of the braided outer conductor reduces and subsequently an inductive distortion occurs on the cable sensor due to the added inductance. The notches were formed perpendicular to the longitudinal axis of the cable sensor and placed with a 25 mm separation. The schematic illustration of the cable sensor is shown in Fig. 1.

This modification does not cause a loss in the uniformity of the cable sensor because the integrity of the outer conductor is not deteriorated. Consequently, the signal loss due to the modification is avoided and monitoring distance is not affected.

3.3 Test set-up, model pile and measurement system

Bending test of piles under monotonic loading is usually conducted for investigating the flexural capacity and cracking behavior of the piles to be considered for determining the correct experimental pile responses and lateral load–displacement curves (Akiyama *et al*. 2012, Chiou *et al*. 2014). In this

(a) The molds used to cast the model piles

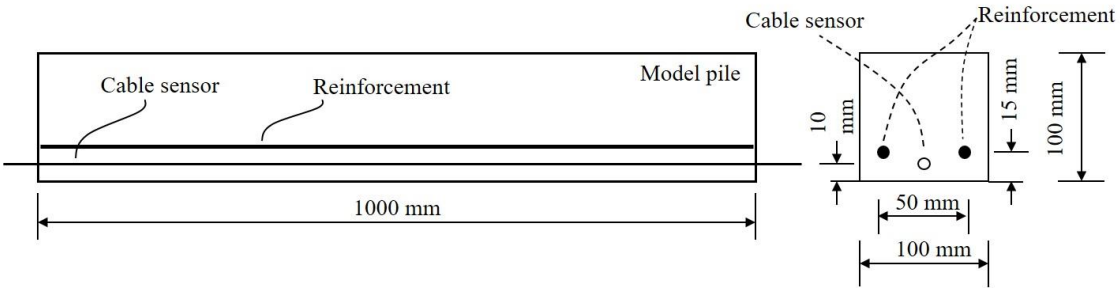

(b) Cross section of the model piles

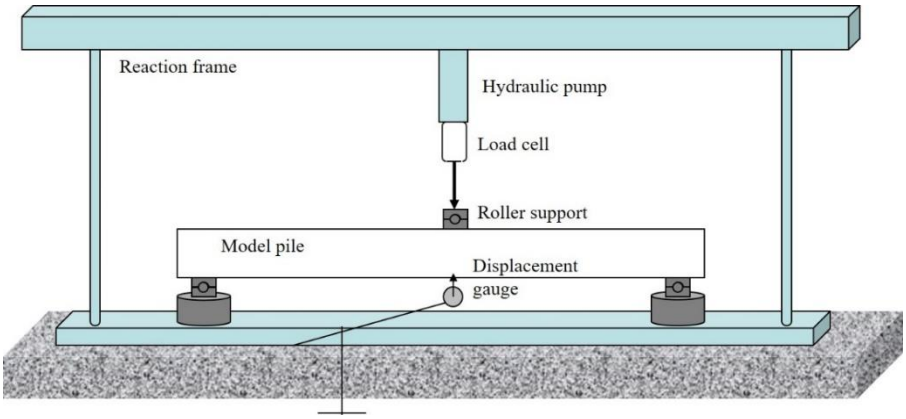

(c) Test setup

Fig. 2 Details of the model piles and the test setup

study, 3-point bending tests were conducted on the model piles with a general-purpose hydraulic test frame in order to validate the usability of the proposed modification approach. The length of the model piles was 1000 mm. The model piles had a square cross section of dimensions 100 mm by 100 mm. Two stainless steel threaded rod of 4 mm diameter were placed 50 mm apart symmetrically about the centerline at a distance of 15 mm to the tension side as longitudinal reinforcement. Model piles were cast without stirrups. Details of the model piles and the sketch of the test set up are shown in Fig. 2. Model piles were cast in steel plate molds using the concrete which was prepared with

Fig. 3 Photograph of the displacement gauge and the observed damage pattern

Table 3 Details of the concrete mix design

Volumetric ratios		Gravimetric proportions				Maximum aggregate dimension	28th day strength (Mean)
water/cement	air/cement	water	cement	coarse aggregate	fine aggregate	10 mm	25 MPa
0.85	6.6	10	11.8	30.7	47.5		

CEM I 42.5 R Portland cement. Maximum dimension of the aggregate was chosen 10 mm according to the similitude laws (10 percent of the biggest dimension of the cross-section). The details of the concrete mix design are tabulated in Table 3.

After 48 hours of casting the concrete, the model piles are demolded and set aside to cure. The steel rods were commercially available (Class A2-70), and their minimum yield and ultimate tensile strengths were reported as 450 MPa and 700 MPa, respectively. The modulus of elasticity (E, based on the compressive strength) and the Poisson's ratio of concrete were calculated as 30 GPa and 0.2, respectively, by the help of Eurocode (2004). The modular ratio (between the modulus of elasticity of the steel rod and that of the concrete) was approximately 8.

The cable sensor was positioned at the centerline of the cross section, precisely 10 mm away from the tension side. It was coated with a thin layer of epoxy based adhesive (The Original Super Glue® SY-SS) before the casting of the concrete for the purpose of achieving proper bonding. This coating also helps to avoid water ingress into the cable sensor through the notches on the protective jacket. The position of the cable sensor was fixed by two spring clamps mounted at the ends of the mold, hence, sagging was avoided.

The monotonic and incremental bending load was applied on a 50 mm wide steel plate at the mid-span of the model pile with manual control. The tests were carried out without a constant

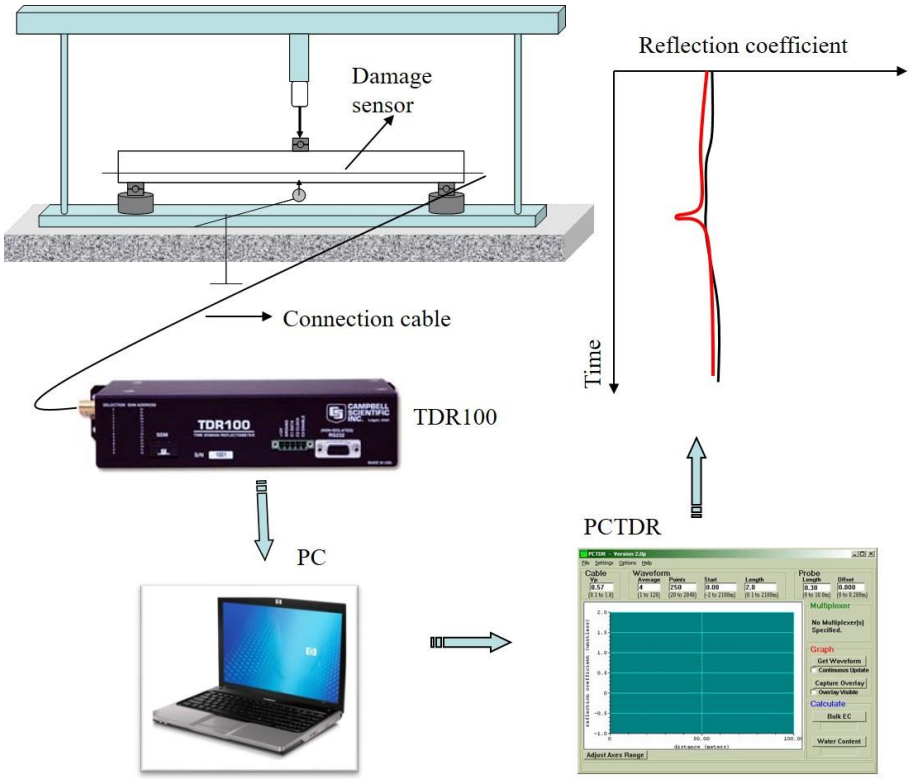

Fig. 4 A sketch of the measurement system

displacement or stress rate. The maximum load was achieved within approximately 8 minutes and the complete test had a duration of 15 minutes. The magnitude of the applied load was measured by a load cell and recorded manually. The displacement at the mid-span of the model pile was determined with a displacement gauge, simultaneously. The progress of the damage pattern was visually observed, and TDR measurements were performed after each load step. A photograph of the displacement gauge and the observed damage pattern is shown in Fig. 3.

A total of 4 model pile specimens were produced (Table 4). Coaxial cables RG59/U-6 and RG6/U-4 with the modification proposed in this study served as the cable sensors in the specimens MP2 and MP4, respectively. MP1 and MP3 were produced with “as is” commercial coaxial cables RG59/U-6 and RG6/U-4, respectively, in order to serve a base to evaluate the performance of the proposed modification for the cable sensors.

The TDR measurement system used in the experimental part of this study is shown in Fig. 4. The cable sensor was connected to the TDR100 via connection cable possessing a 75-ohm impedance. The impedance of this connection cable was selected as the same as that of the cable sensor in order to prevent signal attenuation due to an impedance mismatch. A BNC (Bayonet Neill–Concelman) connector was used for the connection. The resulting waveform, representing the ρ along the cable sensor, displayed with 12.2 picoseconds timing resolution by the PCTDR software. When the α (0.01 Neper, see Table 2) and the total sensor cable length (2.75 m) are considered together in Eq. (4), the A is then calculated as 1.05. So, the ohmic dissipations were negligible for the cable models

Table 4 List of the model pile specimens

Specimen	Coaxial cable	Modification
MP1	RG59/U-6	No
MP2	RG59/U-6	Yes
MP3	RG6/U-4	No
MP4	RG6/U-4	Yes

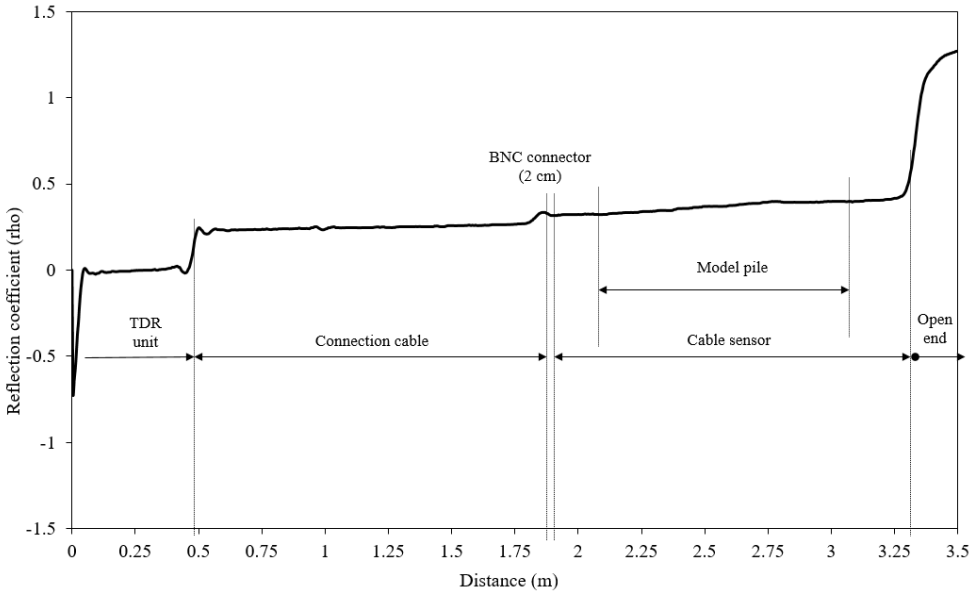

Fig. 5 The reference waveform of the model pile MP3

and length of the cable sensors in this study. When the t_r of the TDR100 and the V_p of the cable sensor were considered together in Eq. (7), the R was 35 mm, while the accuracy of the measurement system was 2.9 mm in accordance with the timing resolution.

A reference waveform was obtained first with TDR100 before the tests were conducted as shown in Fig. 5. The first 50 cm (approximately) of the resulting waveform is the region where the incident test wave was produced and traveled through the inner components of the TDR100. In the connection cable region, the reflection coefficient has a value of 0.23 as can be calculated with Eq. (2). The cable sensor started after the BNC connector and launched out 10 to 25 cm from both ends of the model piles. Finally, the reflection from the open end termination was observed.

4. Results

A representative experimental response (load-displacement) curve of the model piles is shown in Fig. 6. A theoretical calculation based on strain compatibility and force equilibrium was performed for checking the conformity of the experimental response curve.

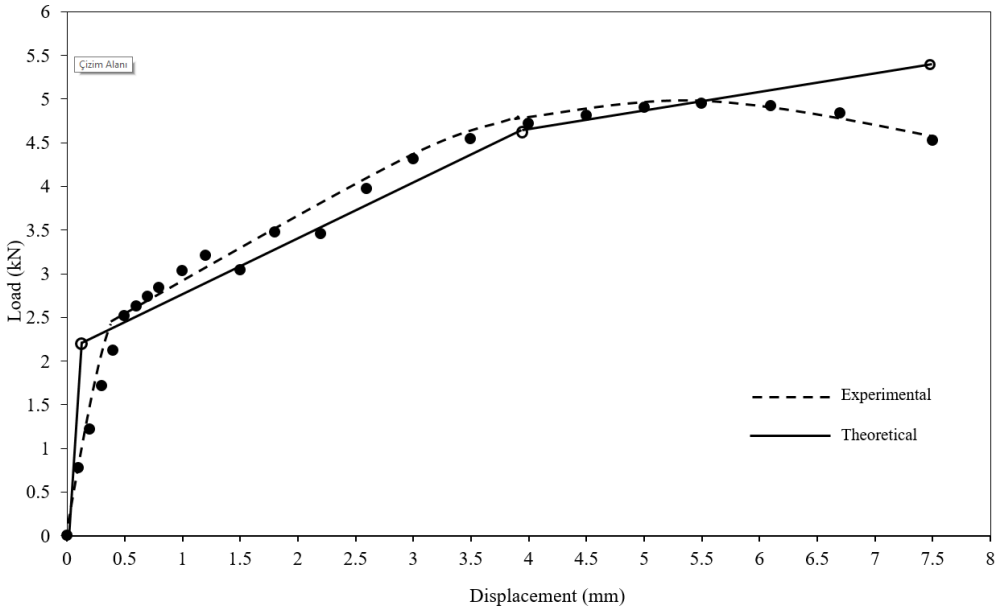

Fig. 6 Load-displacement curve of the model pile MP3

The cracking moment (M_{cr}) of the section was obtained by the help of Eq. (8)

$$M_{cr} = \frac{f_r I_g}{y_t} \tag{8}$$

where f_r is the modulus of rupture of the concrete which can be calculated based on the mean compressive strength of the concrete, I_g is the moment of inertia of the cross section and y_t is the vertical distance from the extreme tension fiber to the neutral axis. Subsequently, the corresponding vertical displacement (δ_{cr}) at the mid-span of the model pile was obtained with Eq. (9)

$$\delta_{cr} = \frac{P_{cr} L^3}{48 E I_g} \tag{9}$$

where P_{cr} is the cracking load which can be obtained from the M_{cr} according to loading configuration and L is the span length. The loads and the corresponding displacements at the yielding and failure stages were calculated with the transformed-area method.

The response curve resulted in a satisfying conformity when compared with the theoretical calculation. The difference between the experimental and theoretical results is mainly due to the lack of additional displacement gauges at the supports for compensating the rigid body translation of the model pile. The distance between the actual and the considered point of quasi-concentrated loading is also an additional source of discrepancy. The initial crack was formed at a force level of 2.5 kN (about 50% of the maximum load).

The deterioration took place nearly about 5.5 mm at a force level of 5 kN for the given model pile.

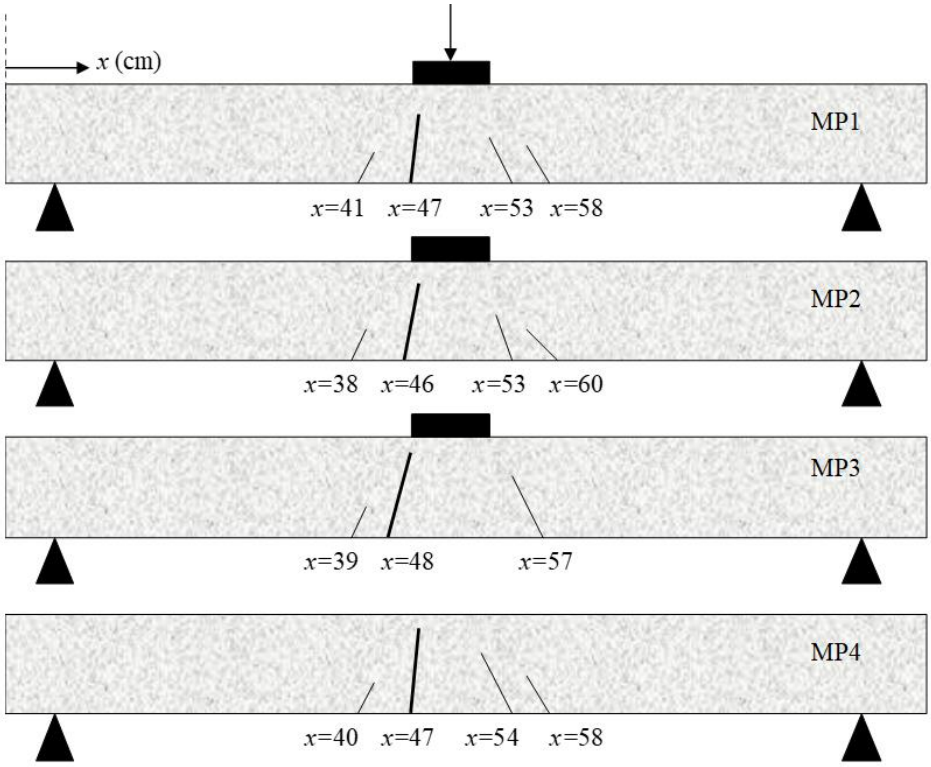

Fig. 7 Crack pattern of the model piles

Positive bending moment resulted a typical cracking behavior under flexure. A compression zone was formed above the neutral axis of the pile section, while the model pile was under tension below the neutral axis. Consequently, the cracks were formed and randomly distributed in the region of maximum bending moment of the tension side. The crack pattern recorded on the one side of the model piles is shown in Fig. 7. One primary crack was observed at the mid-span of the model piles, while additional secondary cracks were formed as the applied load was increased. The width of the cracking area was very limited due to the low reinforcement ratio (0.25%) of the model pile.

4.1 TDR response of RG59/U-6 cable sensor

The model pile MP2 was monitored by modified RG59/U-6 coaxial cable during the 3-point bending tests. The first crack occurred at a force level of 2.5 kN. The corresponding resulting waveform obtained from the cable sensor is shown in Fig. 8. The test region is signed with a dashed line box on the resulting waveform. The primary crack was firstly observed on the resulting waveform with a 0.045 rho variation. As the load was increased, the width of the crack mouth opening displacement (CMOD) increased and resulted in a higher variation in the reflection coefficient. The resulting waveform was approximated to an open end reflection at the failure load. Open end reflection on the cable sensor signs the rupture of the outer conductor of the sensor.

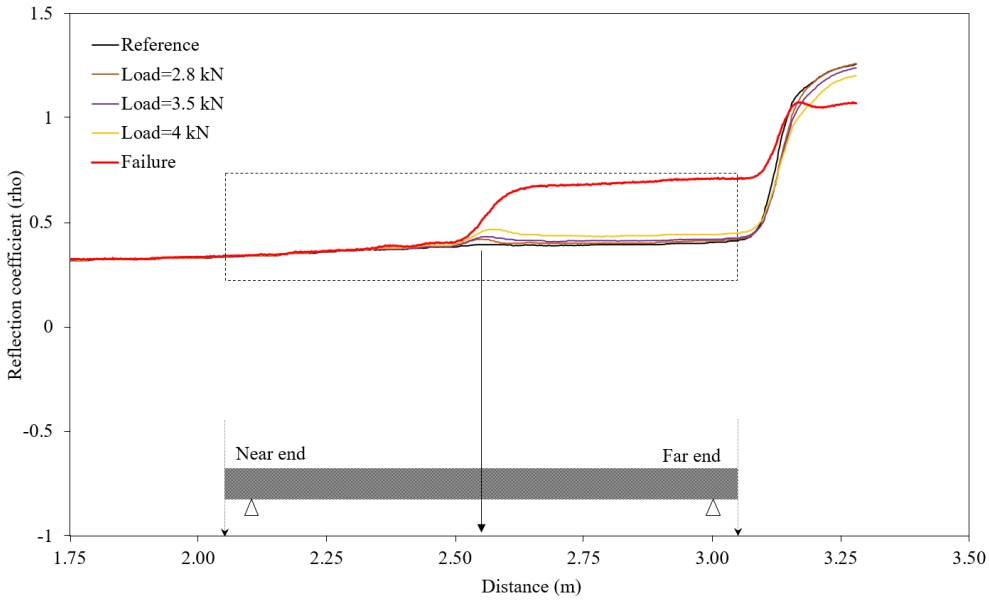

Fig. 8 Resulting waveform of RG59/U-6 cable sensor of MP2

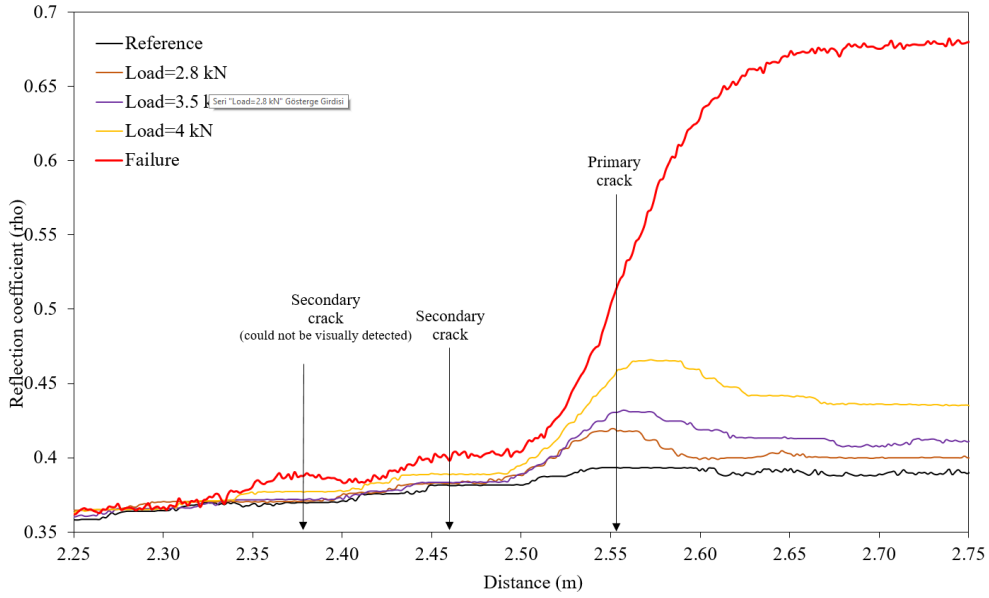

Fig. 9 Closer look to the resulting waveform of RG59/U-6 cable sensor of MP2

A closer look to the resulting waveform of RG59/U-6 cable sensor of specimen MP2 can be seen in Fig. 9. Two secondary cracks before the primary crack can clearly be defined with the help of the variation in the reflection coefficient at the failure load. When the resulting waveform was compared with the crack pattern, the crack locations were determined with 3 cm overestimation partly due to

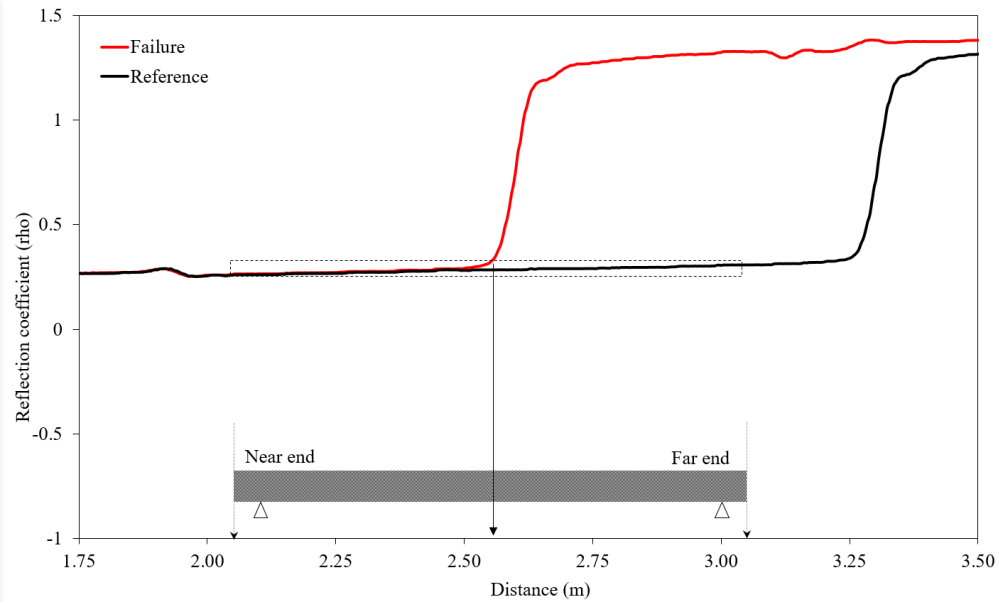

Fig. 10 Resulting waveform of RG6/U-4 cable sensor of MP4

the fact that the damage sensor was located 10 mm above the tension side of the model pile. It should be noted that the cracks which were located after the primary crack could not be distinguished due to the major damage of the outer conductor of the cable sensor at the failure load.

4.2 TDR response of RG6/U-4 cable sensor

The model pile MP4 was monitored by modified RG6/U-4 coaxial cable during the 3-point bending tests. The first crack occurred at a force level of 3.2 kN. The resulting waveform obtained from the cable sensor of MP4 is shown in Fig. 10. None of the cracks was distinguishable with the sensor before the failure of the specimen. Open end reflection was observed at the failure load. It should be noted that the inclination of reflection waveform at the crack location and the end of the cable sensor was the same. This means that the outer conductor of the cable sensor was completely ruptured. The location of the primary crack was determined with 3 cm overestimation.

4.3 Performance of the cable sensors

Resulting waveforms of non-modified commercial coaxial cables RG59/U-6 and RG6/U-4 of MP1 and MP3 at the failure load were utilized in order to evaluate the performance of the cable sensors (see Fig. 11). The resulting waveform was not able to convey information for damage sensing along the test region for both of the coaxial cables. The maximum variation in reflection coefficient was 0.026 rho and 0.007 rho for RG59/U-6 and RG6/U-4, respectively. Remembering the $\pm$3 ohm potential deviation in the characteristic impedance of the coaxial cables, a variation in reflection coefficient under 0.040 rho should be considered as negligible. Although, there were primary and secondary cracks on the model piles, none of them was distinguishable by the ordinary "as is" commercial coaxial cables as expected.

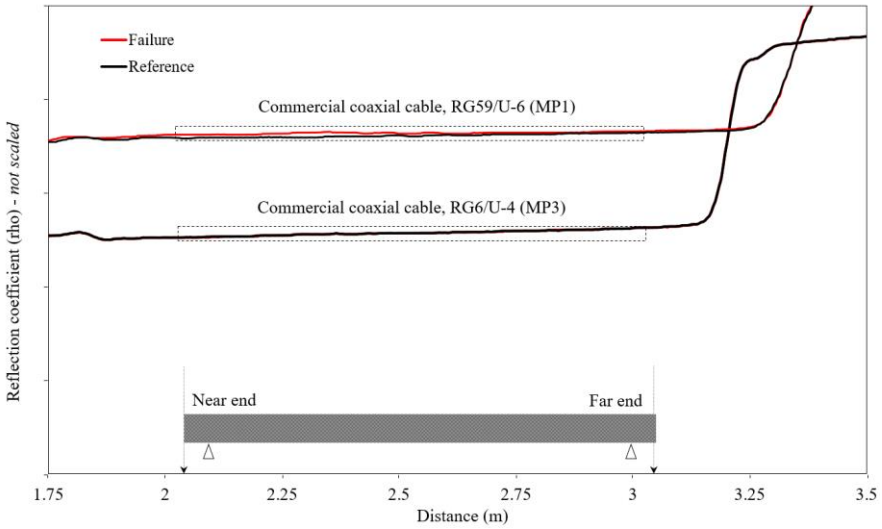

Fig. 11 Resulting waveforms of commercial RG59/U-6 and RG6/U-4 of MP1 and MP3

Table 5 Results of the strain sensitivity analysis

Sensor*	Reference ρ	ρ at 1.60 mm of CMOD	Variation	Variation (%)	Increase in sensitivity
RG59/U-6	0.3775	0.3951	0.0176	4.66	-
RG6/U-4	0.3754	0.3762	0.0008	0.21	-
RG59/U-6 M	0.3787	0.4607	0.0820	21.65	4.65
RG6/U-4 M	0.3712	0.3893	0.0181	4.88	23.24

The variations in the reflection coefficient of the cable sensors and the commercial coaxial cables for the primary crack with a CMOD of 1.60 mm in the test region can be seen for comparison in Fig. 12. It is clear that the variations in the reflection coefficient were under the critical value of 0.040 rho, except for the RG59/U-6 sensor cable. So, the crack was only distinguished by the RG59/U-6 cable sensor. The reflection coefficients corresponding to the CMOD of 1.60 mm are also utilized for strain sensitivity analysis in order to evaluate the performance of the proposed modification approach and the results are tabulated in Table 5. The increase in the strain sensitivity is calculated by dividing the percentage of variation in reflection coefficient of the cable sensors with that of the commercial coaxial cables. As can be seen from Table 5, the RG59/U-6 and RG6/U-4 cable sensors expose approximately 5 and 23 times, respectively, higher strain sensitivity in comparison with non-modified "as is" commercial versions of the cables used. The variation in the reflection coefficient of the RG59/U-6 cable sensor with the increasing CMOD for the primary crack in comparison with that of the study by Zhou *et al.* (2016) can be seen in Fig. 13.

The crack was initially distinguished with a CMOD of 0.4 mm and reached to 1.6 mm at the failure load. As the CMOD increased, the variation in the reflection coefficient was almost linearly increased. This means that the crack development can be monitored by the RG59/U-6 cable sensor with a simple calibration.

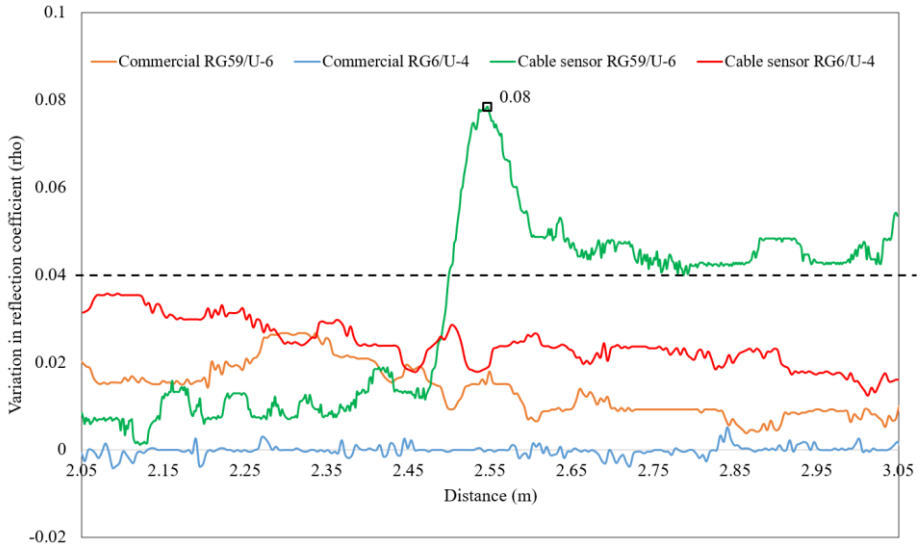

Fig. 12 Variation in reflection coefficient of the cable sensors and the commercial coaxial cables for a crack mouth opening of 1.60 mm

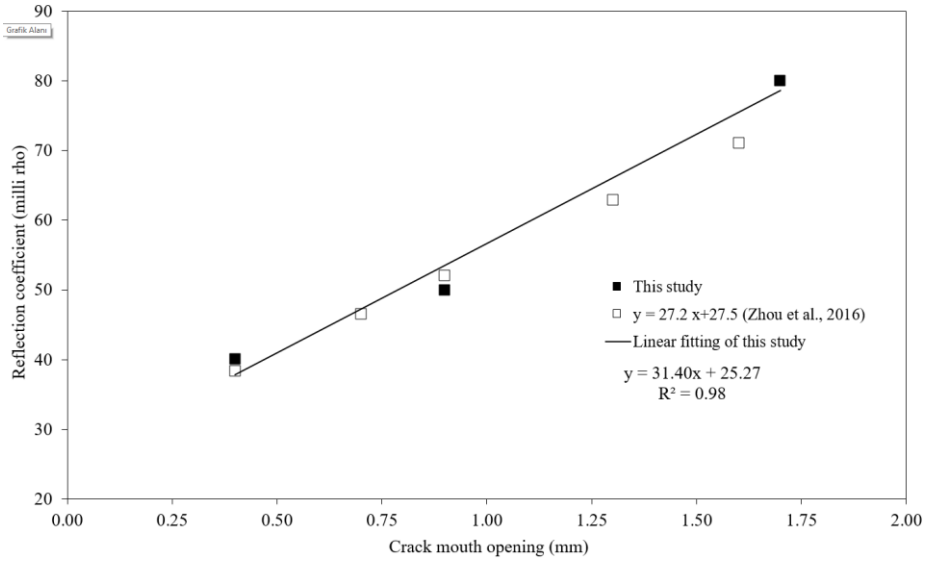

Fig. 13 Variation of reflection coefficient of the RG59/U-6 cable sensor with crack mouth opening

5. Organization of SHM system with TDR

SHM can provide early warning of structural damages that is essential when the damages are just formed (Ho *et al*. 2022). In Fig. 14, a flowchart of the SHM system with TDR as a NDE method for damage assessment of obscured RC structural members is proposed. The first part of the system

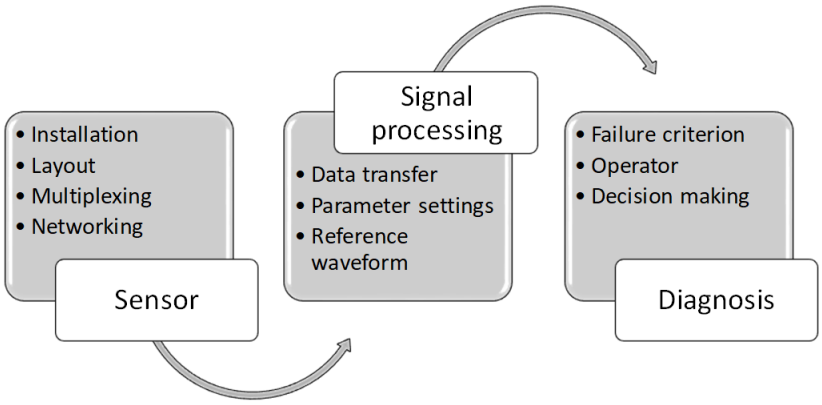

Fig. 14 Flowchart of the proposed SHM system with TDR for obscured structural members

corresponds to the preparation of the sensor. After the installation of the cable sensor to the structural member, it is essential to record the layout and the length of the cable sensor in order to consider signal losses due to the cable length. Multiplexing and networking is optional for remote monitoring of multiple structural members, simultaneously. Signal processing serves as the second part of the system. After connecting the TDR device to a data logger, a software should be used to link the data logger to a computer for storage of the collected data from the cable sensors. In this stage, some key parameters such as V_p of the cable sensor should be set for locating the damage or failure properly. Although the multiplexers are designed to minimize the signal attenuation, disregarding the effect of multiplexing may lead to inaccurate TDR measurements. After setting the parameters, a reference TDR measurement on the cable sensors should be obtained for diagnosis which is the last part of the proposed SHM system. The threshold value of reflection coefficient for crack detection (i.e. 0.040 rho in this study) and failure of the structural member (i.e. open end termination in this study) should be determined previously to create a diagnostic by the operator, controlling the system. The operator should be adequately trained and competent in basic knowledge on TDR for analyzing the recorded data in order to determine and locate the damage or failure. The final leg of the diagnosis is to define the damage severity and subsequently assessing the effects of the damage on structural reliability by high-skilled engineers.

5.1 Limitations

In the case of a structural member failure, the outer conductor of the cable sensor also ruptures and the resulting waveform takes the form of an open end termination. This means that the structural member cannot be monitored afterwards because the cable sensor yields and is sacrificed. In other words, the approach proposed in this study is valid for detecting the first major stress/strain cycle causing the initial structural damage. However, this should not be viewed as a disadvantage because if this is the case then it means that the structural member has suffered a major damage and requires replacement/repair.

The usability of the method is substantially limited with new structures. Forming a core-hole and embedding the cable sensor in a structural member of an existing structure should not be feasible for most of the cases.

Implementation of the cable sensors is another important issue. The cable sensors must be installed before the casting of concrete. To enhance accuracy, practical measures should be taken to prevent the cable sensors from sagging, such as securing them to the reinforcement cage of the structural member or implementing other suitable precautions.

The experimental program has only considered the tension stresses due to bending in the structural members. Although a major percentage of structural damage is expected to be covered, other stress conditions and combinations are not tested; hence, user discretion is advised for stress conditions different from those in this study.

5.2 Durability

The dielectric permittivity of the water is much higher than that of the insulating materials of common coaxial cables such as teflon and polyethylene. In case of obscured structural members located under the water table in soils, a potential of water ingress to cover concrete and subsequently to the cable sensor from the notches on the protective jacket can take place. In this situation, the impedance profile of the cable sensor would be degenerated and miss leading TDR measurements can occur if precautions are not taken.

6. Conclusions

The usability of a practical and novel modification approach for commercial coaxial cables to detect structural damages in obscured structural members via TDR is demonstrated in this study. The proposed approach can be said to be relatively cost-effective because it does not require special cable sensor design and fabrication processes. Additionally, signal losses and consequently a decrease in monitoring distance is prevented by protecting the integrity of the outer conductor.

Coaxial cables RG59/U-6 and RG6/U-4 were modified with the proposed approach and embedded in the model piles representing an obscured structural member. The experimental validation and assessment of the proposed approach was achieved via bending tests of the model piles. Although the boundary conditions of a pile under a foundation is different from a simply supported beam, response of the cable sensor to flexural cracks can be observed with a bending test. It can be noted that the cable sensors exposed significantly higher strain sensitivity, in comparison with their commercial versions by means of the variation in the reflection coefficient at the primary crack with a CMOD of 1.60 mm with the proposed modification approach. Consequently, the modified cable sensors have the capability of sensing both the presence and the location of a structural damage on an obscured structural member with a maximum aberration of 3 cm. The location of the crack corresponds to the local peak of the reflection coefficient if the outer conductor is not broken. On the other hand, when the outer conductor is broken the crack should be located where the reflection coefficient starts to change. Furthermore, the crack development can be monitored by the RG59/U-6 cable sensor with a simple linear calibration. It should be mentioned here that the sensing capability of the cable sensor depends upon the type of the coaxial cable in addition to stress conditions and the level of adhesion between the sensor and the concrete. If the adhesion is inadequate, stress transfer between the sensor and the concrete may be interrupted. Consequently, sensing ability of the cable should be disappeared.

The experimental results also demonstrate that the resulting waveform of the cable sensors does not change back into the reference waveform after the failure. This is highly desirable for SHM

systems in terms of integrity assessment of obscured structural members. For instance, recovery of the cracks on the RC piles under axial compression is a possible scenario after an earthquake. Unlike the other NDE methods, the proposed approach with TDR will be able to detect the damage induced any time even if the cracks recover after developing. The proposed method is also convenient for continuous monitoring of the structural members in real time.

Acknowledgments

The research described in this paper was financially supported by the Scientific and Technological Research Council of Turkey (TUBITAK, Project ID: 108M297). The authors would like to appreciate and acknowledge the funding provided by TUBITAK.

References

Akiyama, M., Abe, S., Aoki, N. and Suzuki, M. (2012), "Flexural test of precast high-strength reinforced concrete pile prestressed with unbonded bars arranged at the center of the cross-section", *Eng. Struct.*, **34**, 259-270. https://doi.org/10.1016/j.engstruct.2011.09.007.

Aktan, A.E., Catbas, F.N., Grimmelsman, K.A. and Tsikos C.J. (2000), "Issues in infrastructure health monitoring for management", *J. Eng. Mech. Div*., **126**(7), 711-724. https://doi.org/10.1061/(ASCE)0733-9399(2000)126:7(711).

Arsoy, S., Ozgur, M., Keskin, E. and Yilmaz C. (2013), "Enhancing TDR based water content measurements by ANN in sandy soils", *Geoderma*, **195-196**, 133-144. https://doi.org/10.1016/j.geoderma.2012.11.019.

Baker, C.N.Jr., Drumright, E.E., Mensah, F.D., Parikh, G. and Ealy, C.D. (1991), "Use of nondestructive testing to evaluate defects in drilled shafts: Results of FHWA research", *Transp. Res. Rec.*, **1331**, 28-35.

Brownjohn, J.M., De Stefano, A., Xu, Y.L., Wenzel, H. and Aktan, E. (2011), "Vibration-based monitoring of civil infrastructure: challenges and successes", *J. Civil Struct. Health Monit.*, **1**(3-4), 79-95. https://doi.org/10.1007/s13349-011-0009-5.

Castiglione, P. and Shouse, P.J. (2003), "The effect of ohmic cable losses on time-domain reflectometry measurements of electrical conductivity", *Soil Sci. Soc. Am. J.*, **67**(2), 414-424. https://doi.org/10.2136/sssaj2003.4140.

Cerny, R. (2009), "Time-domain reflectometry method and its application for measuring moisture content in porous materials: a review", *Measurement*, **42**(3), 329-336. https://doi.org/10.1016/j.measurement.2008.08.011.

Chakraborty, S. and Brown, D.A. (1997), "Evaluation of unknown pile length under existing bridges in Alabama", Report No. IR-97-05; Highway Research Center, Auburn University, Alabama, USA.

Chen, G.D., Mu, H., Pommerenke, D. and Drewniak, J.L. (2004), "Damage detection of reinforced concrete beams with novel distributed crack/strain sensors", *Struct. Health Monit.*, **3**(3), 225-243. https://doi.org/10.1177/1475921704045625.

Chen, G.D., Sun, S.S., Pommerenke, D., Drewniak, J.L., Green, G.G., McDaniel, R.D., Belarbi, A. and Mu, H.M. (2005), "Crack detection of a full-scale reinforced concrete girder with a distributed cable sensor", *Smart Mater. Struct.*, **14**(3), 88-97. https://doi.org/ 10.1088/0964-1726/14/3/011.

Chen, W.H., Hseuh, W., Loh, K.J. and Loh, C.H. (2022), "Damage evaluation of seismic response of structure through time-frequency analysis technique", *Struct. Monit. Maint.*, **9**(2), 107-127. https://doi.org/10.12989/smm.2022.9.2.107.

Chiou, J.S., Lin, C.L. and Chen, C.H. (2014), "Exploring influence of sectional flexural yielding on experimental pile response analysis and applicability of distributed plastic hinge model in inelastic numerical simulation for laterally loaded piles", *Comput. Geotech.*, **56**, 40-49.

https://doi.org/10.1016/j.compgeo.2013.10.007.
Davis, A.G. and Robertson, S.A. (1976), "Vibration testing of piles", *Struct. Eng.*, **54**(6), 7-10.
Ellsworth, D.E. and Ginnado, K. (1991), "Guide for visual inspection of structural concrete building components", Report No. TR-M-91/18; Construction Engineering Research Lab (Army), Champaign, IL, USA.
Eurocode (2004), Design of Concrete Structures. Part 1: General Rules and Rules for Buildings, European Committee for Standardization; Brussels, Belgium.
Fils, P., Jang, S. and Sherpa, R. (2021), "Field implementation of low-cost RFID-based crack monitoring using machine learning", *Struct. Monit. Maint.*, **8**(3), 257-278. https://doi.org/10.12989/smm.2021.8.3.257.
Hassan, U. and Anwar, M.S. (2010), "Reducing noise by repetition: introduction to signal averaging", *Eur. J. Phys.*, **31**(3), 453. https://doi.org/10.1088/0143-0807/31/3/003.
Hearne, T.M., Stokoe, K.H. and Reese, L.C. (1981), "Drilled-shaft integrity by wave propagation method", *J. Geotech. Eng.*, **107**(10), 1327-1344. https://doi.org/10.1061/AJGEB6.0001192.
Ho, D.D., Luu, T.H.T. and Pham, M.N (2022), "Nondestructive crack detection in metal structures using impedance responses and artificial neural networks", *Struct. Monit. Maint.*, **9**(3), 221-235. https://doi.org/10.12989/smm.2022.9.3.221.
Huang, Y.H., Ni, S.H., Lo, K.F. and Charng, J.J. (2010), "Assessment of identifiable defect size in a drilled shaft using sonic echo method: Numerical simulation", *Comput. Geotech.*, **37**(6), 757-768. https://doi.org/10.1016/j.compgeo.2010.06.002.
Large, D. and Farmer, J. (2009), *Broadband cable access networks: the HFC plant*, (1st Edition), Morgan Kaufmann Publishers, Burlington, Massachusetts, USA.
Ledieu, J., De Ridder, P., De Clerck, P. and Dautrebande, S. (1986), "A method of measuring soil moisture by time-domain reflectometry", *J. Hydrol.*, **88**(3-4), 319-328. https://doi.org/10.1016/0022-1694(86)90097-1.
Li, D.Q., Zhang, L.M. and Tang, W.H. (2005), "Reliability evaluation of cross-hole sonic logging for bored pile integrity", *J. Geotech. Geoenviron.*, **131**(9), 1130-1138. https://doi.org/10.1061/(ASCE)1090-0241(2005)131:9(1130).
Lin, C., Tang, S., Lin, W. and Chung, C.C. (2009), "Quantification of cable deformation with time domain reflectometry-Implications to landslide monitoring", *J. Geotech. Geoenviron.*, **135**(1), 143-152. https://doi.org/10.1061/(ASCE)1090-0241(2009)135:1(143).
Lin, M.W. and Thaduri, J. (2006), "Structural deflection monitoring using an embedded ETDR distributed strain sensor", *J. Intel. Mat. Syst. Str.*, **17**(5), 423-430. https://doi.org/10.1177/1045389X06058631.
Lin, M.W., Abatan, A.O. and Zhang, W.M. (1999), "Crack damage detection of concrete structures using distributed electrical time domain reflectometry (ETDR) sensors", *SPIE Proceedings*, **3671**, 297-304. https://doi.org/10.1117/12.348680.
Lin, M.W., Abatan, A.O. and Zhou, Y. (2000), "High-sensitivity electrical TDR distributed strain sensor", *SPIE Proceedings*, **3986**, 463-471. https://doi.org/10.1117/12.388137.
Lin, M.W., Thaduri, J. and Abatan, A.O. (2005), "Development of an electrical time domain reflectometry (ETDR) distributed strain sensor", *Meas. Sci. Technol.*, **16**(7), 1495. https://doi.org/10.1088/0957-0233/16/7/012.
Liu, W., Hunsperger, R.G., Chajes, M.J., Folliard, K.J. and Kunz, E. (2002), "Corrosion detection of steel cables using time domain reflectometry", *J. Mater. Civil Eng.*, **14**(3), 217-223. https://doi.org/10.1061/(ASCE)0899-1561(2002)14:3(217).
Malicki, M.A., Plagge, R. and Roth, C.H. (1996), "Improving the calibration of dielectric TDR soil moisture determination taking into account the solid soil", *Eur. J. Soil Sci.*, **47**(3), 357-366. https://doi.org/10.1111/j.1365-2389.1996.tb01409.x.
Mao, Q., Mazzotti, M., DeVitis, J., Braley, J., Young, C., Sjoblom, K., Aktan, E., Moon, F. and Bartoli, I. (2019), "Structural condition assessment of a bridge pier: A case study using experimental modal analysis and finite element model updating", *Struct. Control Health.*, **26**(1), e2273. https://doi.org/10.1002/stc.2273.
Ni, S.H. and Huang, Y.H. (2013), "Integrity evaluation of PCC piles using the surface reflection method", *Exp. Techniques*, **37**(4), 63-73. https://doi.org/10.1111/j.1747-1567.2012.00832.x.

Ni. S.H., Huang, Y.H., Zhou, X.M. and Lo, K.F. (2011), "Inclination correction of the parallel seismic test for pile length detection", *Comput. Geotech.*, **38**(2), 127-132. https://doi.org/10.1016/j.compgeo.2010.10.002.

Park, H.S., Lee, H.M., Adeli, H. and Lee, I. (2007), "A new approach for health monitoring of structures: terrestrial laser scanning", *Comput. Aided Civ. Inf.*, **22**(1), 19-30. https://doi.org/10.1111/j.1467-8667.2006.00466.x.

Pozar, D.M. (2012), *Microwave engineering*, (4th Edition), John Wiley & Sons, Inc., Hoboken, New Jersey, USA.

Qin, H., Xie, X., Vrugt, J.A., Zeng, K. and Hong, G. (2016), "Underground structure defect detection and reconstruction using crosshole GPR and Bayesian waveform inversion", *Automat. Constr.*, **68**, 156-169. https://doi.org/10.1016/j.autcon.2016.03.011.

Rausche, F., Renkung, S. and Likins, G.E. (1991), "Comparison of pulse echo and transient response pile integrity test methods", *Transp. Res. Rec.*, **1331**, 21-27.

Recber (2023), Coaxial cables; Recber Cable, Tekirdag, Turkey. https://www.recber.com.tr/product-showcase/coaxial-cables/?lang=en

Rizzo, P. and Enshaeian, A. (2021), "Bridge health monitoring in the United States: A review", *Struct. Monit. Maint.*, **8**(1), 1-50. https://doi.org/10.12989/smm.2021.8.1.001.

Stangl, R., Buchan, G.D. and Loiskandl, W. (2009), "Field use and calibration of a TDR-based probe for monitoring water content in a high-clay landslide soil in Austria", *Geoderma*, **150**(1-2), 23-31. https://doi.org/10.1016/j.geoderma.2009.01.002.

Tektronix (2008), *TDR Impedance Measurements: A Foundation for Signal Integrity*, Application Note No. 55W-14601-2, Tektronix Inc., Beaverton, Oregon, USA.

Topp, G.C., Davis, J.L. and Annan, A.P. (1980), "Electromagnetic determination of soil water content: measurements in coaxial transmission lines", *Water Resour. Res.*, **16**(3), 574-582. https://doi.org/10.1029/WR016i003p00574.

Wang, M., Ding, Y., Wan, C. and Zhao, H. (2020), "Big data platform for health monitoring systems of multiple bridges", *Struct. Monit. Maint.*, **7**(4), 345-365. https://doi.org/10.12989/smm.2020.7.4.345.

Yeum, C.M., Choi, J. and Dyke, S.J. (2018), "Automated region-of-interest localization and classification for vision-based visual assessment of civil infrastructure", *Struct. Health Monit.*, **18**(3): 675-689. https://doi.org/10.1177/1475921718765419.

Yu, X. and Yu, X. (2011), "Assessment of an automation algorithm for TDR bridge scour monitoring system", *Adv. Struct. Eng.*, **14**(1), 13-24. https://doi.org/10.1260/1369-4332.14.1.13.

Zhou, Z., Jiao, T., Zhao, P., Liu, J. and Xiao, H. (2016), "Development of a distributed crack sensor using coaxial cable", *Sensors*, **16**(8), 1198. https://doi.org/10.3390/s16081198.

JK